Journal of Solid State Chemistry **167,** 363–369 (2002)
doi:10.1006/jssc.2002.9546

Synthesis, Characterization, and Catalytic Properties of a Microporous/Mesoporous Material, MMM-1

Raja H. P. R. Poladi and Christopher C. Landry[1]

Department of Chemistry, Cook Physical Science Building University of Vermont, Burlington, Vermont 05405

Received October 19, 2001; in revised form February 11, 2002; accepted February 15, 2002; published online April 17, 2002

DEDICATED TO PROFESSOR GALEN STUCKY ON THE OCCASION OF HIS 65TH BIRTHDAY

A microporous–mesoporous material composed of MCM-41 and MFI was produced by a two-step synthetic process. The solid, called "MMM-1," was characterized by X-ray diffraction (XRD), N_2 physisorption, and transmission electron microscopy (TEM). At early stages of crystallization at 170°C, MCM-41 was formed exclusively, while at heating times longer than 96 h MFI was formed. At intermediate times, MMM-1 was formed with varying amounts of MFI depending on the crystallization time. XRD revealed that the material could be severely oriented by sample preparation, which was consistent with an unusual ribbon-like morphology observed in TEM. This morphology was not seen for either pure MCM-41 or MFI. The N_2 physisorption isotherm for MMM-1 showed two distinct regions of capillary condensation, with H2 hysteresis. Synthesis and subsequent use of Al-MMM-1 in the isomerization of *m*-xylene and comparison to Al-MCM-41 and Al-MFI showed that although the latter material had a higher total conversion, Al-MMM-1 had a higher selectivity for *p*-xylene. Al-MMM-1 had a much higher selectivity and conversion than Al-MCM-41, which makes it promising for use in future catalytic applications.

Key Words: **microporous; mesoporous; MFI; MCM-41; MMM-1.**

INTRODUCTION

Zeolites are widely used as cation exchangers, adsorbents and catalysts (1). Their unique activity and use in a growing variety of applications has created interest in the development of novel zeolitic materials with varying pore dimensions, composition, and reactivity. Aluminophosphates (2) and mesoporous materials of the well-studied M41S, (3–6), SBA (7), and other structure types (8), such as MCM-41, are porous materials with larger pore dimensions compared to zeolites and therefore have the potential for reactions of larger molecules. However, the catalytic activity of these materials varies to a great extent, even among the materials with similar compositions, and microporous zeolites such as MFI have shown superior activity compared to large pore molecular sieves (9). Similarly, the incorporation of transition metal ions such as titanium into M41S materials or large pore zeolites does not produce materials as active as TS-1 (Ti-MFI) for the oxidation of organic intermediates (10). Due to its small pore size, TS-1 cannot be utilized in catalytic processes involving larger molecules. Thus, there is incentive to synthesize materials which have larger pore sizes of mesoporous materials and yet retain the catalytic ability of zeolites.

Several reports have appeared on the synthesis of microporous/mesoporous materials. Kloetstra *et al.* have synthesized samples with partial recrystallization of the porous surfaces of mesoporous materials by ion exchange with tetrapropylammonium ions (TPA^+) (11). Huang *et al.* have reported an MCM-41/MFI material in which the percentage of MFI remained small and the product had a disordered structure (12). Attempts to increase the percentage of MFI resulted in the destruction of the mesoporous material. Karlsson *et al.* have reported the synthesis of complex aggregates of MCM-41/MFI materials in which MFI crystals were partially embedded in MCM-41 aggregates (13). Huang *et al.* have used reaction mixtures in which surfactants and TPA^+ were present together in the same reaction to prepare samples with both micro- and mesoporosity (14), and others have used similar methods to synthesize SBA-15/ZSM-5 composites with larger mesopores (15).

In the above studies, the mesoporous material was synthesized first and was subsequently crystallized to produce a microporous phase. More recent studies have shown that it is also possible to work in the opposite direction, namely, to assemble mesoporous materials from zeolite "seeds," yielding a product with both micro- and mesoporosity (16). Interestingly, the latter materials were strongly acidic and were hydrothermally stable even at the high temperatures likely required for practical use. A similarly acidic and

[1]To whom correspondence should be addressed. Fax: (802) 656-8705. E-mail: cclandry@zoo.uvm.edu. Internet: www.uvm.edu/~cclandry.

0022-4596/02 $35.00

catalytically active material has also been prepared by a different method (17).

In this report, we describe the synthesis of MCM-41/MFI materials by a two-step process involving manipulation of the growing mesoporous material under non-equilibrium conditions through the use of an organic additive in the reaction mixture, namely TPA^+. Various characterization techniques are used to characterize the resulting material. The synthetic method allows the content of MFI in the product to be fine tuned to any desired amount between 0 and 100%, depending simply on the length of time that the reaction mixture is crystallized at 170°C. The synthetic method used here is different from those used previously, and yields a material with unusual N_2 physisorption properties and a unique particle morphology.

TABLE 1
Summary of Materials Produced by Varying the Crystallization Time (Heating Time at 170°C)

Crystallization time (hours at 170°C)	Products
0	MCM-41 (weak)
6	MCM-41
9	MCM-41
12	MMM-1
24	MMM-1
36	MMM-1
48	MMM-1
72	Lamellar mesostructure (weak)/MFI
96	MFI

EXPERIMENTAL SECTION

Materials and Methods

NaOH was received from J. T. Baker; all other chemicals were purchased from Aldrich and used as received. Powder X-ray diffraction experiments were performed on a Scintag X1 θ–θ diffractometer equipped with a Peltier (thermoelectrically cooled) detector and using Cu$K\alpha$ radiation. Scans were performed with step sizes of 0.02° and count times of either 0.5, 1.5, or 7 s per point depending upon the sample. Nitrogen adsorption and desorption isotherms were obtained on a Micromeritics ASAP 2010 instrument. Samples were degassed at 200°C under vacuum overnight prior to measurements. Surface area and pore size distributions were calculated using Micromeritics software and the theories of Brunauer, Emmett, and Teller (BET) (18) and Barrett, Joyner, and Halenda (BJH) (19), respectively. FTIR measurements were obtained on a Perkin-Elmer System 2000 FTIR. TEM analyses were performed on either a JEOL 100S or JEOL 100CXZ instrument operating at 100 kV. Samples were prepared by mounting in epoxy resin and microtoming to obtain a thin slice.

Synthesis of MMM-1

MCM-41/MFI materials were typically prepared by dissolving NaOH (0.10 g, 2.5 mmol) and cetyltrimethylammonium bromide (CTAB, 0.30 g, 0.82 mmol) in 40 mL deionized water. Tetraethylorthosilicate (TEOS, 3.85 g, 18.5 mmol) was added to the mixture and stirring was continued for 105 min at ambient temperature. The resulting mixture was stirred and heated at 80°C for 20 min; the volume was reduced by approximately half. Tetrapropylammonium bromide (TPABr, 0.26 g, 1.0 mmol) was added before cooling the mixture to room temperature. The reaction composition including the total amount of water before concentration was 1.0 SiO_2:0.68 Na_2O:0.044 CTA^+:0.054 TPA^+:120 H_2O. Stirring was continued for another 30 min before transferring the mixture to a Teflon-lined Parr autoclave to begin crystallization at 170°C. Samples were heated for the times indicated in Table 1. After crystallization was complete, the products were filtered, washed with deionized water, and dried at 120°C. Calcination to remove the organic cations was accomplished by heating the dried products to 550°C at a rate of 2°C/min followed by a 12 h hold at that temperature. Samples were cooled at the same rate to room temperature.

Synthesis of Al-MMM-1

This procedure was very similar to the one above. NaOH (0.27 g, 6.75 mmol) and cetyltrimethylammonium bromide (CTAB, 0.40 g, 1.10 mmol) were dissolved in 31.4 mL deionized water. Tetraethylorthosilicate (TEOS, 3.89 g, 18.5 mmol) was added to the mixture with stirring. Aluminum sulfate ($Al_2(SO_4)_3 \cdot 18\ H_2O$, 0.39 g, 0.58 mmol) was dissolved in 10 mL of deionized water in a separate beaker and then was added to the reaction mixture. Stirring was continued for 105 min at room temperature. The resulting mixture was stirred and heated at 80°C for 20 min in order to reduce the volume by approximately half. Tetrapropylammonium bromide (TPABr, 0.26 g, 1.0 mmol) was added before cooling the mixture to room temperature. The reaction composition including the total amount of water before concentration was 1.0 SiO_2:0.031 Al_2O_3:0.18 Na_2O:0.067 CTA^+:0.053 TPA^+:120 H_2O. Stirring was continued for another 30 min before transferring the mixture to a Teflon-lined Parr autoclave to begin crystallization at 150°C for 24 h and then at 170°C for 20 h. Samples were collected by filtration, dried, and calcined according to the program used above for MMM-1.

Synthesis of Al-MCM-41

Samples were typically prepared by dissolving NaOH (0.40 g, 10.0 mmol) and cetyltrimethylammonium bromide (CTAB, 0.6 g, 1.65 mmol) in 32 mL deionized water.

Tetraethylorthosilicate (TEOS, 3.85 g, 18.5 mmol) was added to the mixture. Aluminum sulfate ($Al_2(SO_4)_3 \cdot 18\ H_2O$, 0.39 g, 0.58 mmol) was dissolved in 10 mL of deionized water in a separate beaker and was then added to the reaction mixture. Stirring was continued for 105 min at ambient temperature. The resulting mixture was stirred and heated at 80°C for 20 min. The mixture was stirred overnight, then was transferred to a Teflon-lined Parr autoclave to begin crystallization at 150°C for 6–12 h. The reaction composition including the total amount of water before concentration was 1.0 SiO_2:0.031 Al_2O_3:0.27 Na_2O:0.089 CTA^+:130 H_2O. Samples were collected by filtration, dried, and calcined according to the program used above for MMM-1.

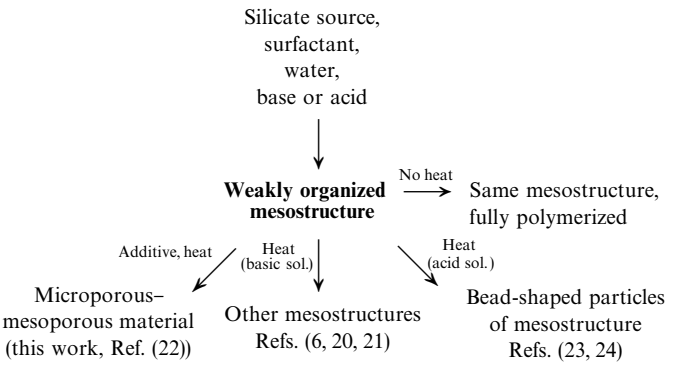

SCHEME 1. Diagram indicating how incompletely polymerized MCM-41 has been used as a starting point for the synthesis of different materials (24).

Synthesis of Al-MFI

Ten grams of colloidal silica (30 wt% SiO_2, 50 mmol), 10 g of TPAOH (1M in water) and aluminum sulfate ($Al_2(SO_4)_3 \cdot 18\ H_2O$, 1.03 g, 1.55 mmol) were added to 10 mL of water. The mixture was stirred for 1 h and then another 7 mL of water was added and the mixture was stirred for another 45 min. The mixture was transferred into Teflon autoclave and crystallization was carried out for 48 h at 170°C. Samples were collected by filtration, dried, and calcined according to the program used above for MMM-1.

Catalytic Studies

The isomerization of *m*-xylene was performed over Al-MMM-1, Al-MCM-41 and Al-MFI in the temperature range 423–573 K in a fixed-bed reactor at atmospheric pressure. The protonated catalysts (1 g), in the form of small pellets, were loaded into a glass reactor and the reactor was flushed with nitrogen at 573 K for 1 h. The reactor was then set to the reaction temperature. *m*-Xylene was passed through the catalyst by passing nitrogen through a bubbler containing *m*-xylene at 298 K (9 mm vapor pressure, 10 cm^3/min). At each temperature the reaction was carried out for 3 h. The products were analyzed every 30 min on-line by an Agilent model 6890 gas chromatograph equipped with a carbowax capillary column and a flame ionization detector.

RESULTS AND DISCUSSION

We have previously published results from experiments in which the mesoporous material MCM-48 was formed from MCM-41 by a phase transformation process (6, 20, 21). This two-step process involved stirring the MCM-41 reaction mixture at room temperature for a short time, and then heating it above 100°C before the MCM-41 was fully polymerized. Ethanol, produced by the hydrolysis of the silicate source tetraethylorthosilicate (TEOS), was shown to alter surfactant packing within the micellar surfactant templates around which the silicate polymerized. The resulting increase in surfactant volume within the micelle was sufficient to cause a phase transformation to MCM-48. It is important to note that changes in the concentrations of the reagents were not required. It was simply the interplay between ethanol, surfactant, and silica at various temperatures that controlled the formation of the products.

The phase transformation process is synthetically attractive because a single reaction mixture can be used to form two different products. The key is the formation of a "weakly organized" silica–surfactant mixture. At early stages of synthesis, the mesostructure is sufficiently organized such that it has an identifiable structure by XRD, yet is still not polymerized enough to withstand calcination. This provides a useful starting point for the formation of other porous solids (Scheme 1). In the study discussed above, ethanol was the "additive" responsible for the phase transformation. At low concentrations, other molecules may also be used to manipulate the mesostructure as it continues to polymerize.

In this study, TPA^+ was added to the reaction mixture when the mesostructure was only weakly organized (Scheme 2). This molecule has been shown to act as a template for the formation of the MFI zeolite structure. The reaction mixture was then transferred to a Parr autoclave and heated at 170°C. The composition was adjusted so that MFI would be formed after heating for 96 h or more, but MCM-41 would be formed if the mixture was not heated at all. At heating times less than 96 h, a material containing both micro- and mesopores was formed. Thus, one reaction mixture could be used to form three different materials depending on the heating time. In this paper, the MCM-41/MFI material is called "MMM-1" (microporous/mesoporous material).

Powder X-Ray Diffraction (XRD)

XRD patterns of MMM-1 crystallized for 6, 12, 24, 36, 48, and 72 h are shown in Figs. 1 and 2. Data are summarized

$$\text{CTAB} + \text{NaOH} + \text{H}_2\text{O} \xrightarrow[\text{Stir 105 min}]{\text{TEOS,}} \xrightarrow[\text{30 min}]{\text{353 K,}} \xrightarrow[\text{Stir 30 min}]{\text{TPABr,}} \xrightarrow[\text{443 K, 1–4 d}]{\text{Crystallize,}} \text{MMM-1}$$

$$\text{CTAB} + \text{NaOH} + \text{H}_2\text{O} \xrightarrow[\text{Stir 105 min}]{\text{Al}_2(\text{SO}_4)_3\text{, TEOS,}} \xrightarrow[\text{30 min}]{\text{353 K,}} \xrightarrow[\text{Stir 30 min}]{\text{TPABr,}} \xrightarrow[\text{423 K, 1 d}]{\text{Crystallize,}} \xrightarrow[\text{443 K, 20 h}]{\text{Crystallize,}} \text{Al-MMM-1}$$

SCHEME 2. Summary of the synthetic procedures used to produce MMM-1 and Al-MMM-1.

in Table 1. As expected, weakly defined MCM-41 with unresolved secondary peaks (3–5°2θ) was formed even before the hydrothermal crystallization had begun. Six hours of crystallization were required to obtain well-defined MCM-41 with three distinct peaks under these synthetic conditions. When crystallization was carried out for longer than 9 h, the secondary peaks of the mesoporous phase decreased in intensity, probably due to a decreased ordering length related to the reaction of TPA^+ with the pore walls. After 12 h, a material showing XRD peaks corresponding to both MCM-41 and MFI had formed. Interestingly, MMM-1 showed a preferred orientation in the (010) direction, as illustrated by the fact that the peaks indexed to (020), (040), and (060) planes of the microporous phase showed unusually high intensities compared to those of normal MFI. Further XRD experiments illustrated that this orientation is due to sample preparation. This type of orientation has not been observed in any previous preparations of microporous/mesoporous materials and appears to be unique to the synthetic method described here (11–17). Since MFI produced by heating the reaction mixture for 72 h or more did not show this orientation, we conclude from the XRD data that the particle morphology of MMM-1 is different from that of MFI. This was investigated further by TEM (vide infra).

The percentage of transformation from MCM-41 to MFI, as determined by the intensities of the MFI XRD peaks relative to the MCM-41 peaks, increased when the crystallization time was increased from 12 to 48 h. A further increase in crystallization time from 48 to 72 h led to the formation of MFI with only small amounts of a mesoporous material present. The ordering of the peaks in the mesoporous region of the spectrum was indicative of a lamellar structure, leading to the conclusion that significant breakdown of the MCM-41 had occurred. As expected, the lamellar mesophase collapsed upon calcination. At this stage, the MFI had also lost its orientation. The relationship between the orientation of the MFI and the presence of MCM-41 suggests that the MFI phase is not formed as separate silica particles but uses MCM-41 as its source, transforming it into MMM-1 before consuming it completely.

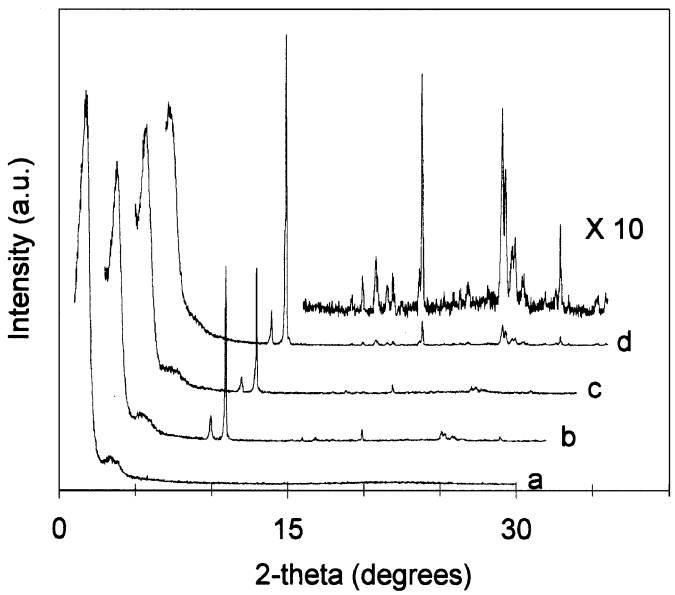

FIG. 1. X-ray diffraction patterns of calcined MMM-1 crystallized at 170°C for various times: (a) 6 h; (b) 12 h; (c) 24 h; (d) 36 h.

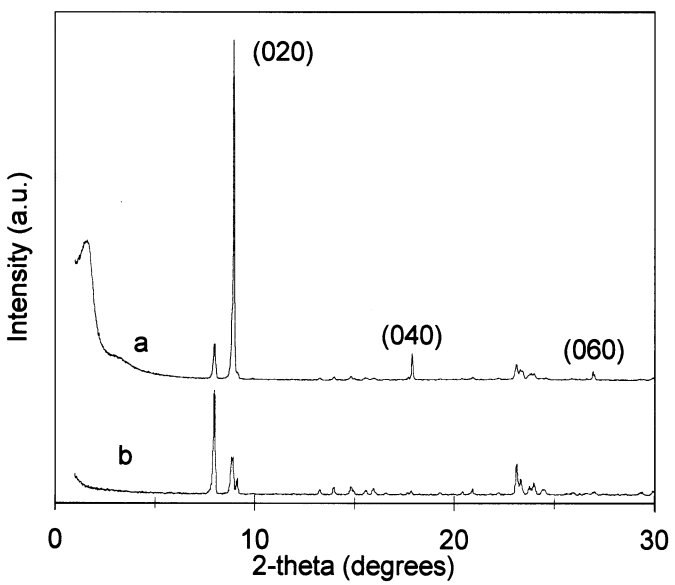

FIG 2. X-ray diffraction patterns of calcined MMM-1 crystallized at 170°C for (a) 48 h and (b) 72 h.

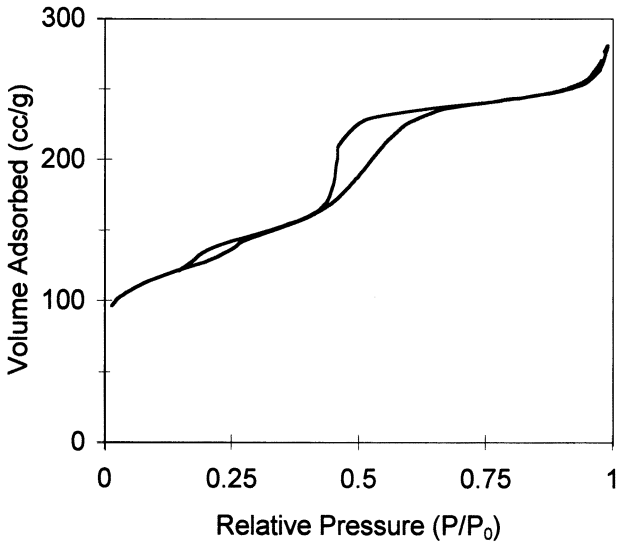

FIG. 3. Nitrogen adsorption and desorption isotherms of MMM-1 crystallized at 170°C for 48 h.

Although the TPA^+ did not appear to alter the MCM-41 peak positions and hence pore sizes, heating the reaction mixture for successively longer and longer times did cause a shift in the d_{100} peak from 2.1°2θ to lower angles. This indicates a gradual increase in mesopore size as the sample is heated at 170°C, a result that is in agreement with studies from other groups who also heated mesoporous phases in basic solution (25).

Nitrogen Physisorption

N_2 physisorption isotherms for MMM-1 exhibited two regions of hysteresis between the adsorption and desorption traces, from relative pressures (P/P_o) of 0.15–0.30 and 0.50–0.70 (Fig. 3). The hysteresis at the relative pressure range of 0.45–0.60 is similar to Type IV isotherm initially described by Brunauer (18), although it occurs at lower relative pressure than expected and the overall shape of the isotherm is different. Such hysteresis has been shown to occur in mesoporous samples simply due to the nature of capillary condensation in larger pores, i.e. above ~ 40 Å in diameter (26). However, this type of hysteresis (H2) is also thought to be due to the presence of an "inkwell" pore geometry in which the mouth of the pore is smaller than its diameter. The pore geometry may be responsible for the enhancement of the hysteresis in this region of the isotherm. Again, this type of isotherm has not been observed in microporous/mesoporous materials prepared by other methods.

The smaller H2 hysteresis at P/P_o of 0.15–0.30 is more unusual. Normally, isotherms of M41S materials that exhibit capillary condensation in this region do not show hysteresis. This step in the isotherm is most likely due exclusively to the inkwell pore geometry, with mesopores connecting to smaller pore geometries. Analysis of physical mixtures of MCM-41 and MFI with varying ratios produced isotherms with very similar shapes, but none of the physical mixtures showed hysteresis in this region. The overall conclusions to be drawn from the porosity analysis are that MMM-1 samples contain a variety of micro- and mesopores of different geometries. While it is tempting to state that the samples described here contain interconnected networks of micro- and mesoporous, this point cannot be proven conclusively by physisorption without further studies.

Transmission Electron Microscopy (TEM)

Figure 4 presents the TEM images of MMM-1 crystallized for 9, 24, and 36 h. At 9 h, MMM-1 exhibited a well-ordered mesoporous pore structure, confirmed by XRD. As the crystallization time was increased to 12 h, ribbon-like

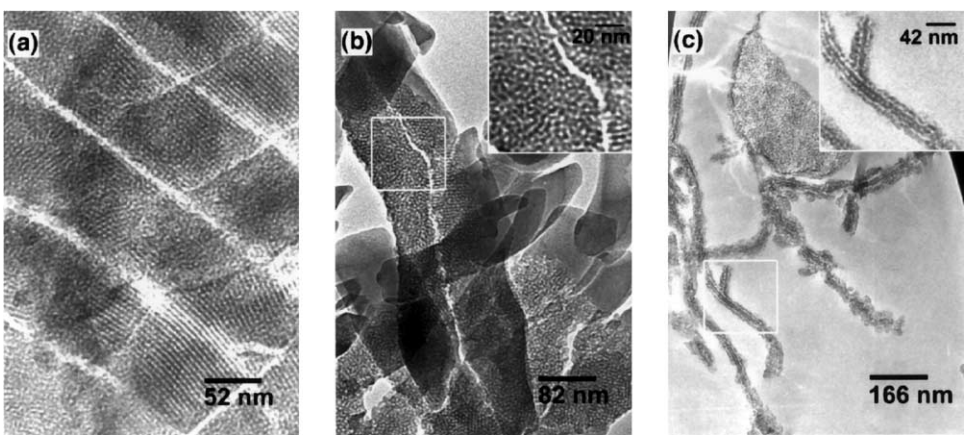

FIG. 4. Transmission electron microscopy images of MMM-1 crystallized at 170°C for various times: (a) 9 h; (c) 24 h; (d) 36 h.

shapes began to appear in the vicinity of the MCM-41 pores. This particle morphology has only been reported once before for an MFI/MCM-41 material (14). At this stage, XRD showed peaks of both MCM-41 and MFI. The simultaneous observance of these structures and oriented MFI peaks in XRD suggests that they are related, and that the ribbons are regions of microporous growth. Preferred orientation due to sample preparation can also be observed for layered clays, which have a similar particle morphology in that they are elongated in one dimension. Longer crystallization times (24 h and longer) produced large blocks that ultimately attained shapes identical to those of MFI produced by other methods. At these stages, the mesoporous material became increasingly disordered as shown by the lack of striations in the TEM images due to the mesoporous structure. By 36 h, mesoporous regions could be identified but no organized regions similar to those shown in the 9 h MMM-1 remained. This pore structure is similar to the "wormhole" structures described for the MSU and APMS mesoporous materials (8, 23, 27). The major particle morphologies at this stage were ribbons and blocks. MMM-1 heated for 72 h showed only the block morphology, corresponding to the XRD spectrum (Fig. 2b) that showed only non-oriented MFI.

m-Xylene Isomerization

Al-containing MMM-1 was prepared by a method similar to that used to prepare the siliceous MMM studied above (Scheme 2). Aluminum sulfate was used as the Al source, and the Si/Al ratio was approximately 16. For comparison, Al-MFI (ZSM-5) and Al-MCM-41 were prepared using the same sources and with the same Si/Al ratios. The three samples were then used for the isomerization of *m*-xylene, an industrial process in which MFI is typically used. The results are shown in Fig. 5. As expected, Al-MFI clearly had a higher total conversion than Al-MMM-1, and Al-MCM-41 showed almost no conversion at all. However, Al-MMM-1 showed a higher selectivity for *p*-xylene than Al-MFI, and also showed a slightly higher preference for the formation of the desired isomerization products (*p*- and *o*-xylene) than disproportionation products (toluene and trimethylbenzenes). Al-MMM-1 had very similar catalytic activity to Al-MFI, and was distinctly different from Al-MCM-41 in its activity. It therefore promises to be an interesting substrate for further catalytic studies. In related studies, we have also shown that Ti-MMM-1 had a higher total conversion for the oxidation of alkanes, and was more selective for ketone and alcohol products, than either TS-1 (Ti-MFI) or Ti-MMM-1 (22).

CONCLUSIONS

Materials comprised of microporous MFI and mesoporous MCM-41 were prepared using a two-step, two-template synthetic method. Weakly organized MCM-41 was transformed to MFI before it had completely polymerized. The extent of transformation was controlled by the crystallization

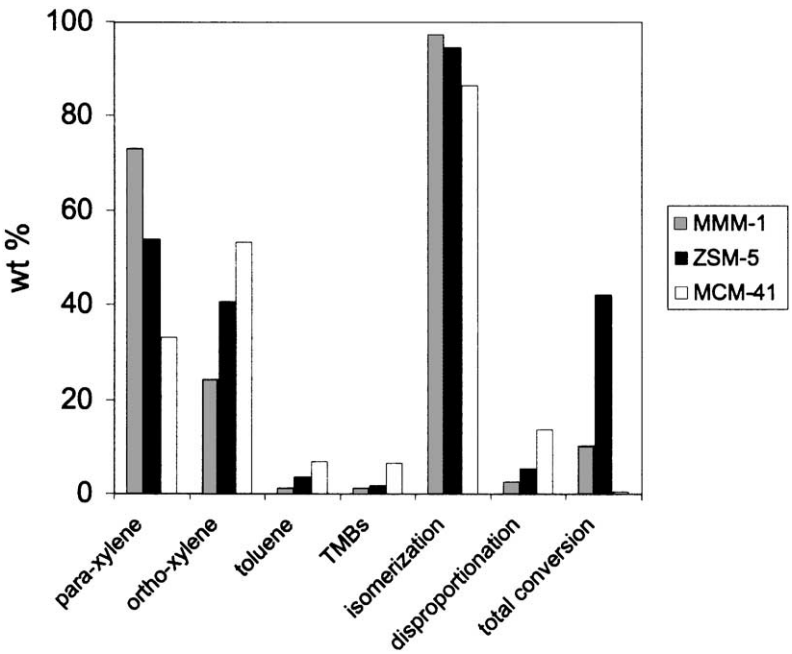

FIG. 5. Product distributions from the reaction of *m*-xylene with Al-MMM-1, Al-MCM-41, and Al-MFI. Reaction temperature = 473 K; contact time = 6.22 h.

time. At short crystallization times, the MFI peaks of the microporous/mesoporous material, studied by XRD, showed a preferred orientation due to sample preparation. TEM of MMM-1 showed an unusual particle morphology, and N_2 physisorption experiments suggested the presence of interconnected pore structures. A comparison of *m*-xylene isomerization by Al-MMM-1, Al-MCM-41, and Al-MFI showed that Al-MMM-1 is distinctly more active than the pure mesoporous phase, although it has a lower total conversion than Al-MFI.

ACKNOWLEDGMENTS

This research was supported by the NSF through a CAREER award (CHE-9875768) and also by the University of Vermont. The authors thank Dr. Russell Morris for useful discussions and Joseph Moore for assistance in obtaining TEM images.

REFERENCES

1. R. Szostak, "Molecular Sieves—Principles of Synthesis and Identification." Van Nostrand Reinhold, New York, 1989.
2. S. T. Wilson, B. M. Lok, C. A. Messina, T. R. Cannan, and E. M. Flanigen, *J. Am. Chem. Soc.* **104,** 1146 (1982).
3. (a) C. T. Kresge, M. E. Leonowicz, W. J. Roth, J. C. Vartuli, and J. S. Beck, *Nature* **359,** 710 (1992); (b) J. S. Beck, J. C. Vartuli, W. J. Roth, M. E. Leonowicz, C. T. Kresge, K. D. Schmitt, C. T.-W. Chu, D. H. Olson, E. W. Sheppard, S. B. McCullen, J. B. Higgins, and J. L. Schlenker, *J. Am. Chem. Soc.* **114,** 10,834 (1992).
4. (a) Q. Huo, D. I. Margolese, U. Ciesla, D. G. Demuth, P. Feng, T. E. Gier, P. Sieger, A. Firouzi, B. F. Chmelka, F. Schüth, and G. D. Stucky, *Chem. Mater.* **6,** 1176 (1994); (b) Q. Huo, D. I. Margolese, U. Ciesla, P. Feng, T. E. Gier, P. Sieger, R. Leon, P. M. Petroff, F. Schüth, and G. D. Stucky, *Nature* **368,** 317 (1994).
5. (a) M. T. Janicke, C. C. Landry, S. C. Christiansen, D. Kumar, G. D. Stucky, and B. F. Chmelka, *J. Am. Chem. Soc.* **120,** 6940 (1998); (b) M. T. Janicke, C. C. Landry, S. C. Christiansen, S. Britain, G. D. Stucky, and B. F. Chmelka, *Chem. Mater.* **11,** 1342 (1999).
6. K. W. Gallis and C. C. Landry, *Chem. Mater.* **9,** 2035 (1997).
7. (a) Q. Huo, R. Leon, P. M. Petroff, and G. D. Stucky, *Science* **268,** 1324 (1995); (b) D. Zhao, J. Feng, Q. Huo, N. Melosh, G. H. Frederickson, B. F. Chmelka, and G. D. Stucky, *Science* **279,** 548 (1998); (c) D. Zhao, Q. Huo, J. Feng, B. F. Chmelka, and G. D. Stucky, *J. Am. Chem. Soc.* **120,** 6024 (1998); (d) Z. Luan, M. Hartmann, D. Zhao, W. Zhou, and L. Kevan, *Chem. Mater.* **11,** 1621 (1999).
8. (a) S. A. Bagshaw, E. Prouzet, and T. J. Pinnavaia, *Science* **269,** 1242 (1995); (b) P. Tanev and T. J. Pinnavaia, *Science* **271,** 1267 (1996); (c) S. A. Bagshaw, T. Kemmitt, and N. B. Milestone, *Microporous Mesoporous Mater.* **22,** 419 (1998).
9. A. Corma, *Chem. Rev.* **97,** 2373 (1997).
10. (a) P. Tanev, M. Chibwe, and T. J. Pinnavaia, *Nature* **386,** 239 (1994); (b) J. C. van der Waal and H. van Bekkum, *J. Mol. Catal.* **124,** 137 (1997).
11. K. R. Kloetstra, H. van Bekkum, and J. C. Jansen, *Chem. Commun.* 2281 (1997).
12. L. Huang and Q. Li, *in* "Proceedings of the 12th International Zeolite Conference" (M. M. J. Treacy, B. K. Marcus, M. E. Bisher, and J. B. Higgins, Eds.). MRS Press, Warrendale, PA, 1998.
13. A. Karlsson, M. Stocker, and R. Schmidt, *Microporous Mesoporous Mater.* **27,** 181 (1999).
14. L. Huang, W. Guo, P. Deng, Z. Xue, and Q. Li, *J. Phys. Chem. B* **104,** 2817 (2000).
15. D. T. On and S. Kaliaguine, *Angew. Chem. Int. Ed. Engl.* **40,** 3248 (2001).
16. (a) Y. Liu, W. Zhang, and T. J. Pinnavaia, *Angew. Chem. Int. Ed. Engl.* **40,** 1255 (2001); (b) Y. Liu, W. Zhang, and T. J. Pinnavaia, *J. Am. Chem. Soc.* **122,** 8791 (2000).
17. Z. Zhang, Y. Han, L. Zhu, R. Wang, Y. Yu, S. Qiu, D. Zhao, and F.-S. Xiao, *Angew. Chem. Int. Ed. Engl.* **40,** 1258 (2001).
18. S. Brunauer, P. H. Emmett, and E. Teller, *J. Am. Chem. Soc.* **60,** 309 (1938).
19. E. P. Barrett, L. G. Joyner, and P. P. Halenda, *J. Am. Chem. Soc.* **73,** 373 (1951).
20. C. C. Landry, S. H. Tolbert, K. W. Gallis, A. Monnier, G. D. Stucky, P. Norby, and J. C. Hanson, *Chem. Mater.* **13,** 1600 (2001).
21. S. H. Tolbert, C. C. Landry, G. D. Stucky, B. F. Chmelka, P. Norby, J. C. Hanson, and A. Monnier, *Chem. Mater.* **13,** 2247 (2001).
22. R. H. P. R. Poladi and C. C. Landry, *Microporous Mesoporous Mater.* **52,** 11 (2002).
23. K. W. Gallis, J. T. Araujo, K. J. Duff, J. G. Moore, and C. C. Landry, *Adv. Mater.* **11,** 1452 (1999).
24. K. W. Gallis, A. G. Eklund, S. T. Jull, J. T. Araujo, J. G. Moore, and C. C. Landry, *Stud. Surf. Sci. Catal.* **129,** 747 (2000).
25. D. Khushalani, A. Kuperman, G. A. Ozin, K. Tanaka, J. Garcès, M. M. Olken, and N. Coombs, *Adv. Mater.* **7,** 842 (1995).
26. P. A. Webb and C. Orr, "Analytical Methods in Fine Particle Technology," Micromeritics Instrument Co., Norcross, GA, 1997.
27. C. Boissière, M. Kümmel, M. Persin, A. Larbot, and E. Prouzet, *Adv. Func. Mater.* **11,** 129 (2001).